

# Geometric Evaluation of GeoTIFF Worldview-2 Image Data Acquired Over Sea of Marmara

Gurcan Buyuksalih<sup>1</sup>, Cem Gazioglu<sup>2</sup>, Karsten Jacobsen<sup>3</sup>

<sup>1</sup> Institute of Marine Science and Management, Istanbul University - gurcanb@istanbul.edu.tr

<sup>2</sup> Institute of Marine Science and Management, Istanbul University - cemga@istanbul.edu.tr

<sup>3</sup> Institute of Photogrammetry and GeoInformation, Leibniz Universität Hannover, Germany - jacobsen@ipi.uni-hannover.de

**Keywords:** Marine Environment, WorldView-2, satellite orientation, GeoTIFF geometry, data acquisition

## Abstract

A WorldView-2 GeoTIFF image was used to analyse the potential information for marine application in the Sea of Marmara and the surrounding land. The first problem to be solved was scene orientation, as the GeoTIFF image was not an ortho image but a simple projection to the sea level. The Rational Polynomial Coefficients (RPC) provided with the image did not match the delivered image; orientation by 3D-transformation was required and successful. The possibility of obtaining depth information by stereoscopic survey and the use of radiometric information related to the water depth are explained with some examples. A typical problem when using images is the total reflection of the sun light by the water surface, which is magnified by small waves. This requires images taken in the opposite direction of the sun. In general, the depth information is limited by water turbidity.

## 1. Introduction

### 1.1 Geometric Conditions

A WorldView-2 GeoTIFF is used for marine applications and for mapping parts of the coastal area. Both applications require a geolocation accuracy of about 2m, corresponding to applicable topographic maps. Based on own experience in other areas, the relative accuracy of Google Earth is in the range of 1.5 m up to 2 m in an area covering the entire WV-2 scene. 20 clearly to be identified tie points between the WV2-image and Google Earth could be used as GCP. These GCP were used to check the geometry of the WorldView-2 GeoTIFF. A GeoTIFF image should have the geometry of an ortho-image and should match the GCP, but this was not the case. For this reason, the image geometry was checked with the delivered Rational Polynomial Coefficients (RPC), using bias corrected RPC orientation. This lead to an unsatisfactory result. A 3D-affine transformation solved the orientation problems.

### 1.2 Bathymetric Use

The Institute for Photogrammetry and GeoInformation at the Leibniz University Hannover has carried out an internal study on geoinformation in shallow water from aerial and satellite images (Jacobsen 2005, 72 pages). In this study, the different methods for determining water depth information from images are analyzed and described.

The classic photogrammetric method is the stereo measurement of water depth. Like the grey value dependence of water depth, it depends on the transparency of the water. This is described by the Secchi depth, i.e. the water depth up to which a black-and-white disk is visible from the water surface (Figure 1). The transparency of the water can vary greatly depending on the turbidity in the water. The turbidity material may be sediment from flowing water and/or algae influenced by the nutrient content.

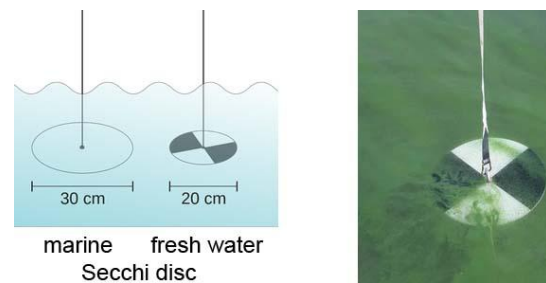


Figure 1. Secchi disc (courtesy of USGS).

If the seabed is homogeneous and the turbidity content is uniform, the water depth can be determined from the gray values of the remote sensing images. However, this also requires a sufficient visibility into the water. Another indication of the depth of shallow water is the use of the wave structure. This can be used to interpolate the water depth over larger distances.

## 2. Image Geometry

The WorldView-2 image used has an angle of incidence of 33.3°. This is the nadir angle from the ground to the satellite, which is larger than the nadir angle of the satellite due to the curvature of the Earth. The GSD is enlarged from 41 cm in nadir view to 49cm x 59 cm, which is changed to 50cm GSD in the available GeoTIFF-image in the ORS2A format.

Ground control points are required for the geometric analysis. The local determination of GCP is time consuming, so Google Earth images were used. In own experience, Google Earth has a standard deviation of the horizontal ground coordinates of about 1.5 m. This is sufficient for the purpose used. Clearly identifiable points must be used. Under optimal conditions, the points should have a symmetric shape and lie a flat plane. Building corners should be avoided due to problems with the object height and shifts caused by illumination changes. In the project area, it is difficult to find such points and compromises are necessary. A typical point used is shown in Figure 2. The centre of the pier is symmetrical, but the crossing water line still represents an edge, also with small differences in height.



Figure 2. Ground control point. Upper right: Google Earth, Upper left and lower: WorldView-2.

The ORS2A-format was initially not specified, so the image geometry had to be analysed. 20 GCP were available, but these were not optimally distributed due to large water surfaces.

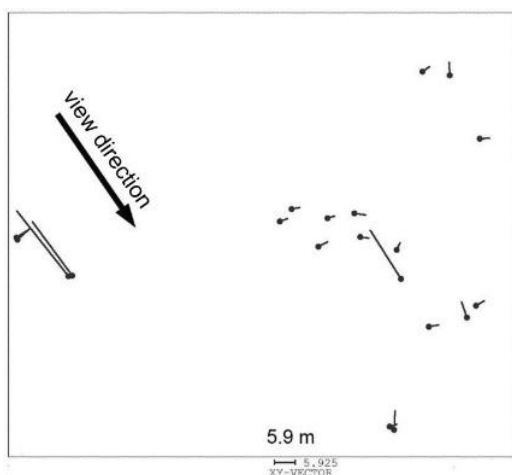


Figure 3. Discrepancies at GCP by direct use of GeoTIFF geometry.

In Figure 3, the discrepancies in X and Y of 3 GCP are noticeable. The vectors based on the direct use of the GeoTIFF geo-reference are in the direction of view of the satellite and have an elevation of 31m, 24m, and 26m, while 4 GCP have an elevation of 6m and the others 1m and 2m respectively above sea level. The horizontal dislocations of 24m, 19m and 17m, together with the elevation, are close to the tangent of the angles of incidence, and clearly show that the available image is just a projection onto the sea level.

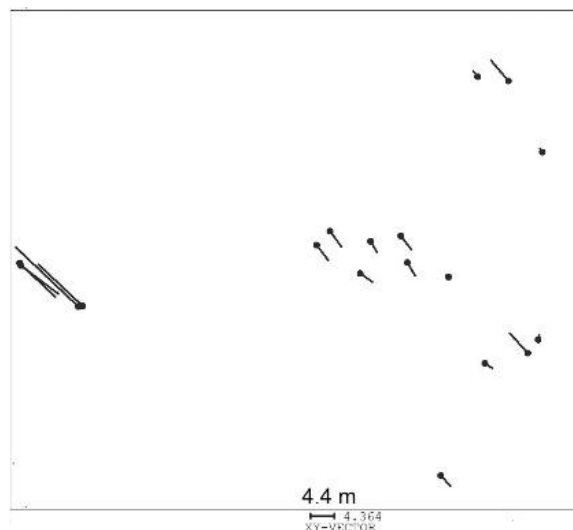


Figure 4. Discrepancies at GCP based on bias corrected RPC.

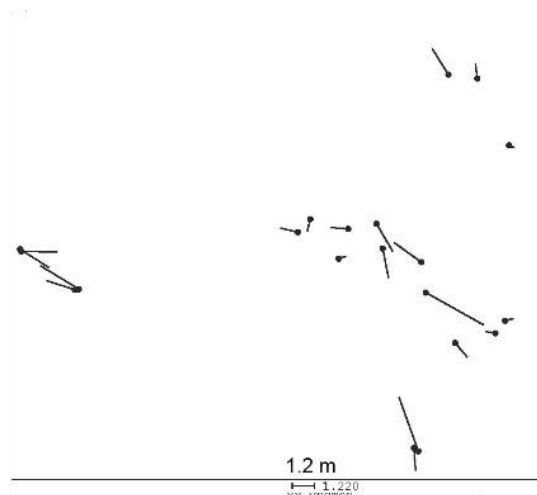


Figure 5. Discrepancies at GCP of 3D-affine transformation (different vector scale as for above discrepancies).

	SX	SY	Number of GCP
Direct use of GeoTIFF	5.11 m	6.64 m	20
RPC all GCP	4.86 m	6.64 m	20
3D-affine transformation	1.30 m	1.23 m	20

Table 1. Results of image orientation.

The bias corrected RPC-orientation, with the RPC delivered together with the image, is also not successful (Figure 4, Table 1). Obviously, these are the RPC belonging to the original WV-2 image and not to the GeoTIFF image. By theory and in reality the 3D-affine transformation can solve the geometric problems. The results based on the 3D-affine transformation (Figure 5 and Table 1, last row) are in line with the expectations. When using GCP based on Google Earth, the standard deviations in X (SX) and Y (SY) are even better than expected at 1.30 m and 1.23 m, respectively and meet the required 2 m.

The common formula for the 3D-affine transformation is (1).

$$\begin{aligned} x_{ij} &= a_1 + a_2 * X + a_3 * Y + a_4 * Z \\ y_{ij} &= a_5 + a_6 * X + a_7 * Y + a_8 * Z \end{aligned} \quad (1)$$

where  $x_{ij}$  and  $y_{ij}$  are the image coordinates,

X, Y, Z = ground coordinates and a1 – a8 the orientation unknown's.

This formula (1) (Hanley et al. 2002) represents an approximation in which parallel lines are used for the viewing directions instead of perspective view in the CCD-line. Geometric differences also occur in the orbit direction, if the change in the viewing direction does not correspond to the speed of the satellite relative to the earth curvature or, in extreme case, in reverse scan direction related to the orbit. With the additional unknown's a9 up to a12, these problems can be respected by Formula (2).

$$x_{ij} = a1 + a2 * X + a3 * Y + a4 * Z + a9 * X * Z + a10 * Y * Z \quad (2)$$

$$y_{ij} = a5 + a6 * X + a7 * Y + a8 * Z + a11 * X * Z + a12 * Y * Z$$

(Büyüksalih et al. 2008).

Extended 3D-Affine Transformation.

The field of view of the WorldView-2 camera is 1.28°. The original GSD in nadir view direction is 41 cm. The perspective view direction against a parallel view direction, corresponding to Formula (1), leads to a dislocation of 1.0 GSD in the line direction, at the end of the line, for a height difference against the reference plane of 36 m (GSD / tan(1.28° / 2.)). For the required accuracy of 2m, a height difference against the reference plane of 179 m is tolerable when applying the simplified Formula (1). Such height differences do not exist in the project area, so the simplified Formula (1) is applicable.

### 3. Bathymetry

The depth of deep water is usually determined using multi-beam echo sounders. For shallow water, profiling echo sounders are used. Such data acquisition is time consuming. Remote sensing can be an alternative solution in shallow water area. Clear water can be penetrated with laser scanners that operate in the green spectral range to a depth that depends on the turbidity of the water. In extreme cases, stereoscopic methods can be used up to a water depth of 30m. The grey values of single images can also provide information about the water depth. For flowing waters in the tidal area, Synthetic Aperture Radar (SAR) can be used for refinement and interpolation over longer distances.

#### 3.1 Transmission, Absorption, and Reflection of Electromagnetic Radiation in Water

Figure 6 gives an overview on the intensity of the solar radiation at ground level. It depends on the solar energy and the penetration through the atmosphere. Terrestrial radiation is important for under water information together with the absorption by the water body. The absorption of water increases significantly in the near infrared range. Water surfaces therefore appear dark to black in the near infrared. The infrared range is therefore not suitable for optical water depth determination. Pure water has much better penetration and reflection at shorter wavelengths. At a wavelength of 680 nm, 35% and at 720 nm, 65% of the incident light is absorbed in pure water alone (Schwoerbel 1999). However, the optimal wavelength for penetrating water must be seen in conjunction with the available solar energy (Figure 6).

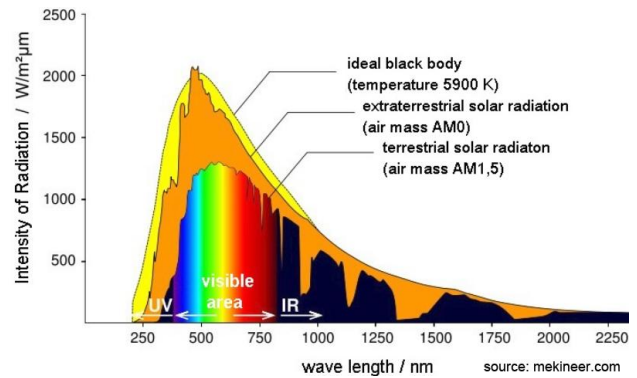


Figure 6. Intensity of sun radiation.

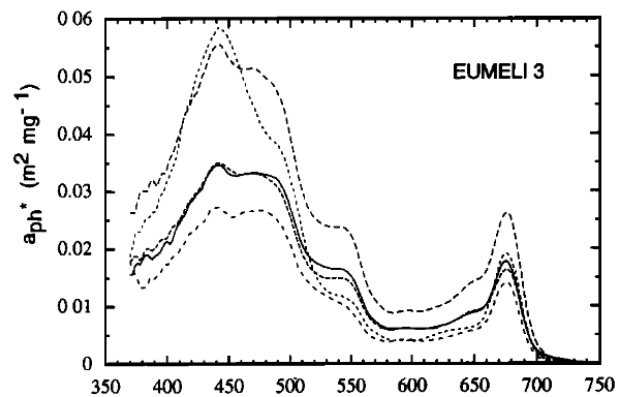


Figure 7. Absorption by phytoplankton as function of wavelength [nm] (Bricaud et al. 1995).

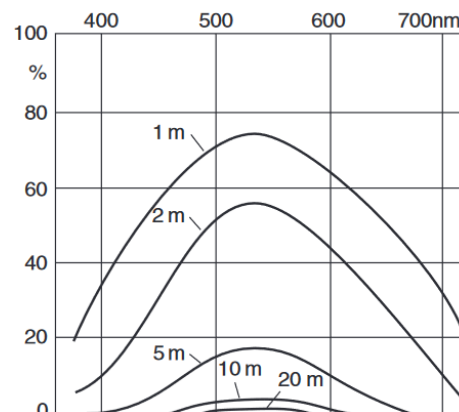


Figure 8. Intensity and spectral composition of light at different depth of sea (Schwoerbel 1999).

The wavelength of the solar radiation intensity, the absorption by phytoplankton (Figure 7) and the absorption of the water (Figure 8) result in a narrow window for optical shallow water survey at a wavelength of approximately 530 nm (green). For this reason, the bathymetric LiDAR scanner use a wavelength of 550nm and it is often used for bathymetric optical survey. The WorldView-2 coastal band (400 – 450 nm) is usable for clear water, but when we have a higher percentage of phytoplankton, the green band (510 – 580 nm) offers advantages.

Space images looking towards the sun (Figure 9, right) must be avoided. Such images with total reflection are useless for stereoscopic measurements. The problems also occurs even if the mirror effect is not exact, as the typical small waves cause additional interference by reflecting the sun light (Figure 10). A

stereo pair with a lower and a higher nadir angle, both facing opposite to the sun, is preferable.

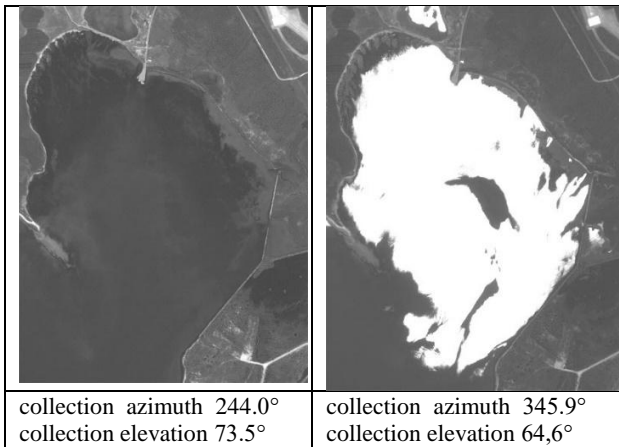


Figure 9. Total reflection in IKONOS stereo scene, Bizerte.

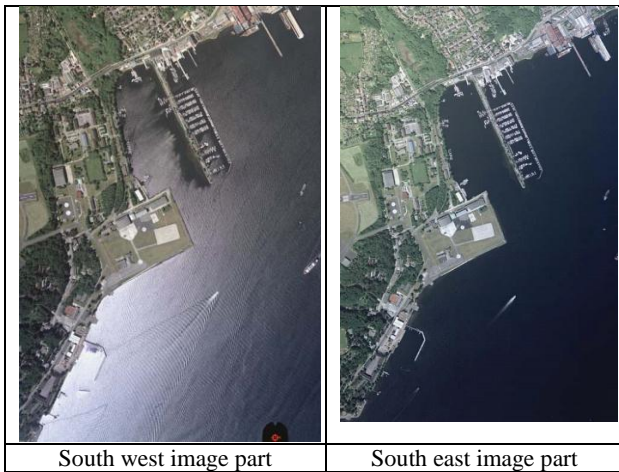


Figure 10. Aerial stereo model affected by total reflection.

When taking aerial images for shallow water surveys, a flight line perpendicular to the sun direction should be preferred. The reflection at the water surface (R), more precisely the bidirectional reflection, is defined as the quotient of the upward radiation below the water surface (Eu) to the downward radiation below the water surface (Ed) (3).

$$R = \frac{Eu}{Ed} \quad \text{Reflectance} \quad (3)$$

The reflectance can go up to total reflectance (mirror effect) and is strongly depending on the wave structure.

### 3.2 Stereoscopic Survey of Shallow Water

When optically surveying of shallow water, the refraction index of the water must be taken into account (Figure 11). As shown, the refraction index depends on the water temperature and the salinity.

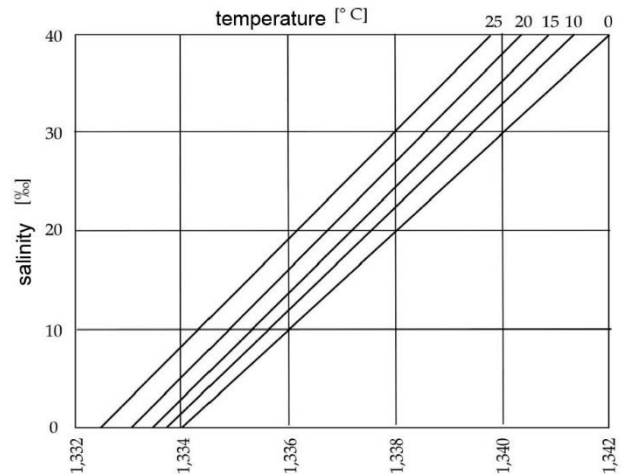


Figure 11. Index of refraction in water.

$$n_A \cdot \sin 1A = n_W \cdot \sin 1W \quad \text{Snellius law about refraction (4)}$$

Where  $n_A$  = refraction coefficient in air (~ 1.0)  
 $n_W$  = refraction coefficient in water  
 $1A$  = angular against plumb direction in air  
 $1B$  = angular against plumb direction in water

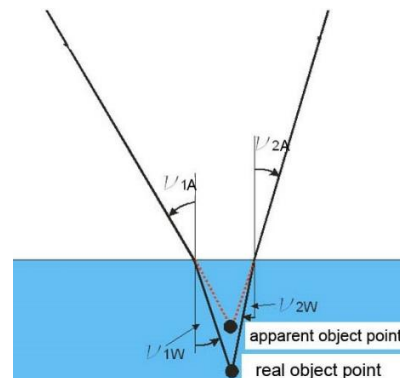


Figure 12. Influence of refraction to water depth.

As shown in Figure 12, the apparent water depth is smaller than the real water depth.

$$\begin{aligned} Z2 / Z1 &= \text{real water depth} / \text{apparent water depth} \\ Z1 &= dpx' / \tan \beta \quad Z2 = dpx' / \tan \beta' \\ Z2 / Z1 &= \tan \beta' / \tan \beta \\ \frac{Z2}{Z1} &= \frac{\sqrt{1 - \sin^2 \beta}}{\sqrt{\frac{1}{n^2} - \sin^2 \beta}} \quad \text{relation real to apperent depth (5)} \\ n &= \text{refraction index} \quad \beta = \text{incidence angle} \end{aligned}$$

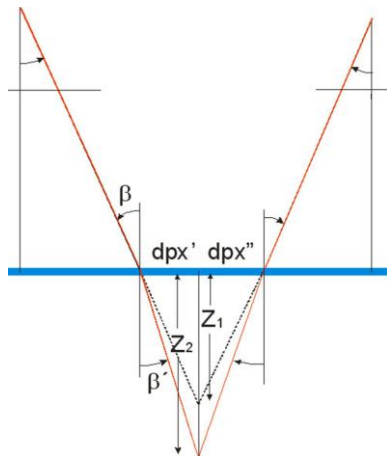


Figure 13. Geometric relationship of underwater points.



Figure 16. Manually measured depth points (red points) in part of the IKONOS stereo scene Bizerte.

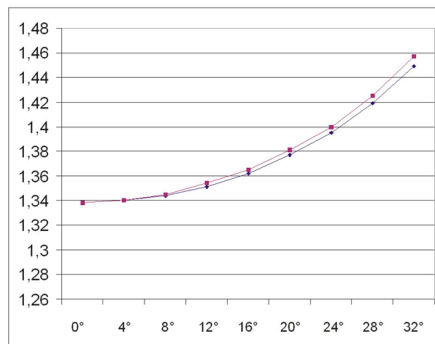


Figure 14: Ratio of real depth to apparent depth of a nadir WorldView-2 image to an inclined satellite image as a function of the angle of incidence of water refraction  $n_W = 1.338$ .

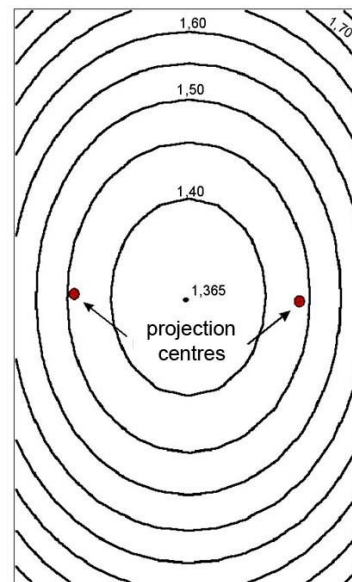


Figure 17. Ratio of real to apparent water depth in the aerial stereo model used at Kiel Bay.

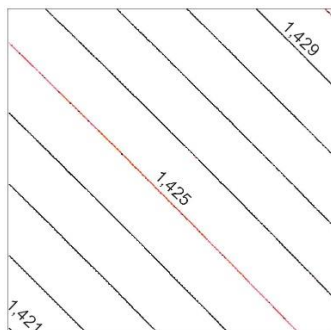


Figure 15: Ratio of real depth to apparent depth in an IKONOS stereo pair for  $n_W = 1.338$  for angle of incidence =  $20^\circ$ , view from southwest, lines perpendicular to viewing direction

Due to the field of view, there is a small variation in the ratio of real to apparent water depth (Figure 14) in satellite images, but the variation of the ratio is within the standard deviation of the measurement. Figure 15 also confirms this.

Due to problems with total reflection, only parts of the IKONOS stereo scene Bizerte could be used (Figure 22). Finally, only 128 points could be manually measured in the blue channel close to the shoreline that had satisfactory reference points in the nautical chart. However, in water depth up to 12 m, a standard deviation of 1.67 m was reached. A higher accuracy was not expected with the 1m GSD of IKONOS and the difficult determination of the reference depth in the nautical chart.

A test with aerial images in the Kiel Bay of the Baltic Sea, had also problems with total reflection. However, due to the 80% overlap in the direction of flight, image combinations with limited influence of the solar reflection could be used. The water depth measurement required manual pointing due to interference from waves on the water surface. An automatic image matching failed. The measurements were only possible in areas with satisfactory contrast on the sea floor. Pure sand areas had to be excluded, but this was only the case for a small percentage of the area. Due to the turbidity, points with a depth down to 5 m below sea level could be determined. Based on the Hannover program "Water", the ratios of real depth to the apparent depth were calculated individually (Figure 17), taking into account the individual image orientation. With a standard deviation of 20 cm, the same accuracy was achieved for the points on sea floor as for the points on land.

#### 4. Radiometric Information for Water Depth

In addition to the geometric determination of water depth, radiometric information can also be used. This is possible if there is sufficiently uniform reflection from the seabed and a

homogeneous turbidity. However, this is not the case near a river mouth. It can be successfully close to small islands. (Mandlbürger et al. 2021) successfully used this method for small groundwater supplied lakes using RGBC (red, green, blue, coastal blue) aerial images. However, it is more difficult in shallow seawater. In general, it depends on the radiative transfer of light in water as function of the water depth and angle of incidence, which increases the path in the water. In addition, wave kinematics and subsurface structure must be taken into account. It varies for different data types (Al Najjar et al. 2023). The relationship water depth and grey values can be determined empirically or by simulation using finally also empirical data. The relationship can change depending on the sun elevation and the direction of view. Finally, the satellite images used may need to be enhanced by a band-pass filter in the range of ocean-specific wavelengths (Al Najjar et al. 2023) (Figures 6 – 8). The complex situation is a typical example for the use of machine learning and deep learning.

Own experience was not very successful. The main problem was the non-homogenous seabed. A typical example where the radiometric information did not lead to successful results is shown in Figure 18. The water surface in Figure 18 is heavily enhanced to identify the cause for the problems in this area. Deep water is expected to correspond to darker water surface colour, however here the turning basin with a depth of 14.5 m (location A) is brighter than the very shallow site B with a water depth of 1.2 m. This is caused by the sea surface. In the turning basin, the sea surface is sucked down, removing the dark algae, while the shallow part B is covered with dark algae. In addition, the water is very clear. The other parts do not meet expectations either. The sea channel C with a depth of 10.5 m is darker on the left side than on the right side, where it is very bright. The sea channel with a depth of 5 m (location D) has similar grey values to the much deeper turning basin.

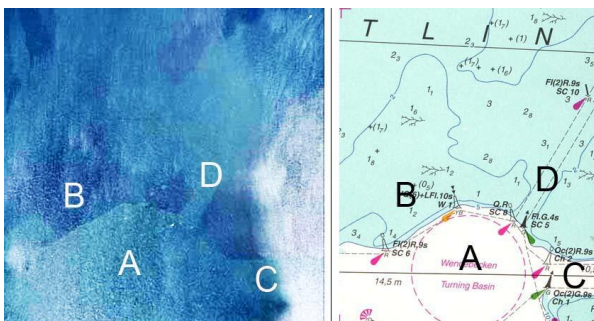


Figure 18. Left: enhanced water surface, right: nautical chart.

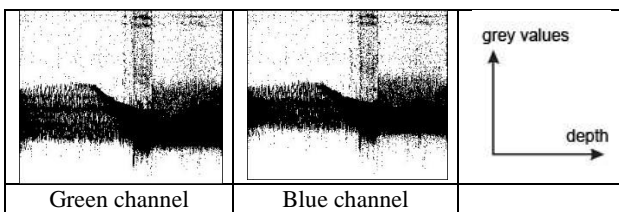


Figure 19. Relationship of water depth and grey values for image shown in Figure 18. Left side: 14.5 m depth Right side: 0.0 m.

The graphical representation of the dependence of the grey values on the water depth in Figure 19 confirms the problem of a missing dependence of the grey values on the water depth.



Figure 20. Relationship of water depth and grey values. Left: 6.35 m depth Right: 0.0 m.

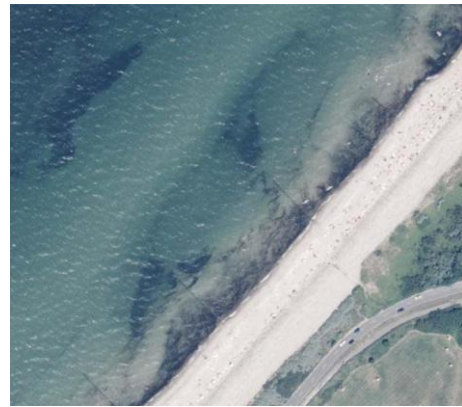


Figure 21. Coastal area with varying seabed.

In the area shown in Figure 20 there is a small dependence of depth on the grey values, but in the deeper part (left) the grey values are brighter and from sea level to a depth of 2.3 m (right side in Figure 20 right) there is a lot of noise caused by the coast line (see also Figure 21).

At the coast line (Figure 21), with highly varying seabed, partly with sandy underground and partly with different algae species, there is no dependency of the grey values on the depth.

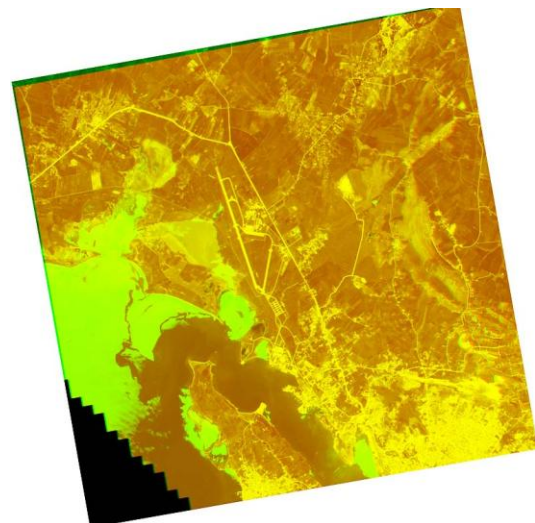


Figure 22. Improved IKONOS anaglyphic stereo model Bizerte.

Figure 22 shows the IKONOS anaglyphic stereo model of Bizerte. The bright homogenous parts are caused by total reflection. So only, a limited part of the water surface can be used stereoscopically.

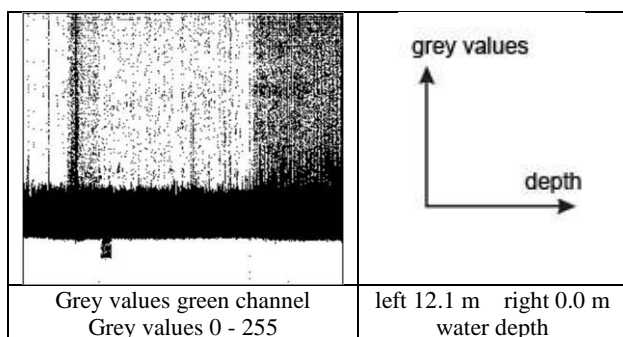


Figure 23. Relation of water depth and grey values, IKONOS, Bizerte.

The right image is not influenced by total reflection and was used after grey value reduction to 8 bit (256 grey values) for the relationship of the water depth from the original grey values of the IKONOS image of Bizerte (Figure 23). Given the experience of above study, it was no surprise that there is no clear dependency. Shipping routes are also being dredged in the area under investigation and the seabed has been disturbed by the shipping traffic.

## 5. Conclusion

The WorldView-2 GeoTIFF image in the ORS2A-format used represents only a projection at sea level. It requires a 3D-affine transformation for the geometrically correct handling of parts that are not at sea level. Based on the 3D-transformation with ground control points from Google Earth, a satisfactory standard deviation of 1.3 m was achieved. Due to the limited height range in the project area, the simple 3D-transformation can be used. For the incidence angle of  $33.3^\circ$  and the required accuracy of 2 m, the extended formula for 3D-transformation (2) is required if the height differences compared to the reference height exceed 179m.

Stereoscopic determination of the water depth using optical images is limited by the turbidity of the water. It requires sufficient contrast on the seabed. Solar reflection must be avoided, which is possible by stereo pairs facing the opposite side of the sun with different angles of incidence. Under optimal condition, almost the same accuracy as for points located on land surface can be reached.

Determine the water depth based solely on grey values of the image is very difficult and only successful when the seabed is very homogenous and the turbidity is uniform across the entire area. The relationship between the water depth and grey values varies with the angle of incidence.

## Acknowledgements

We would like to thank the Centre for Geoinformation of the German Armed Forces for their support in conducting the water depth analysis.

## References

- Al Najar, M., Thoumyre, G., Bergsma, E., Almar, R., Benschila, R., Wilson, D., 2023. Satellite derived bathymetry using deep learning. *Mach Learn*, 112, 1107–1130. doi.org/10.1007/s10994-021-05977-w.
- Bricaud, A., Babin, M., Morel, A., Claustre, H., 1995. Variability in the chlorophyll-specific absorption coefficients of natural

phytoplankton. Analysis and parameterization. *Journal of Geophysical Research*, 100(C7).

Büyüksalih, G., Jacobsen, K., 2008. Digital Height Models in Mountainous Regions based on Space Information. *EARSeL Workshop Remote Sensing - New Challenges of High Resolution*, Bochum.

Hanley, H.B., Yamakawa, T., Fraser, C.S., 2002. Sensor Orientation for High Resolution Imagery. *Pecora 15 / Land Satellite Information IV / ISPRS Archives*, XXXIV, part 1.

Mandlbürger, G., Kölle, M., Nübel, H., Sörgel, U., 2021. BathyNet. A deep Neural network for water depth mapping from multispectral aerial images. *PFG – Journal of Photogrammetry, Remote Sensing and Geoinformation Science*, 89, 71-89.

Schwoerbel, J., 1999. *Einführung in die Limnologie*. Gustav Fischer Verlag, Stuttgart.